



# Late Holocene pteropod distribution across the base of the south-eastern Mediterranean margin: the importance of the > 63 µm fraction

Valentina Beccari<sup>1</sup>, Ahuva Almogi-Labin<sup>2</sup>, Daniela Basso<sup>3</sup>, Giuliana Panieri<sup>4</sup>, Yizhaq Makovsky<sup>5</sup>, Irka Hajdas<sup>6</sup>, and Silvia Spezzaferri<sup>1</sup>

<sup>1</sup>Department of Geosciences, University of Fribourg, Chemin Du Musée 6, 1700, Fribourg, Switzerland

<sup>2</sup>Geological Survey of Israel, Jerusalem, 32 Yesha'ayahu Leibowitz, 9692100, Israel

<sup>3</sup>Department of Earth and Environmental Sciences, University of Milano – Bicocca, CoNISMa, ULR of the University of Milano-Bicocca, Piazza della Scienza 4, 20126, Milan, Italy

<sup>4</sup>Department of Geosciences, CAGE–Centre for Arctic Gas Hydrate, Environment and Climate, UiT The Arctic University of Norway in Tromsø, 9037 Tromsø, Norway

<sup>5</sup>Dr. Moses Strauss Department of Marine Geosciences and Hatter Department of Marine Technology, Leon H. Charney School of Marine Sciences (CSMS), University of Haifa, Haifa, 3498838, Israel

<sup>6</sup>Laboratory of Ion Beam Physics, Swiss Federal Institute of Technology Zurich, 8093 Zurich, Switzerland

**Correspondence:** Silvia Spezzaferri (silvia.spezzaferri@unifr.ch)

Received: 25 October 2022 – Revised: 8 February 2023 – Accepted: 9 February 2023 – Published: 17 March 2023

**Abstract.** Euthecosomata pteropods were analysed in core sediments collected in the framework of the 2016 EUROFLEETS2 SEMSEEP cruise, offshore of Israel, in the eastern Mediterranean Sea. The investigated cores were retrieved in a deep-sea coral area at 690 m depth, an actively methane-seeping pockmark area at 1038 m depth, and a deep-sea channel area at 1310 m water depth. We identified and documented the pteropod species belonging to the families Heliconoididae, Limacinidae, Creseidae, Cavoliniidae, Cliidae, and Hyalocylidae and to some heteropods. Our study highlights the importance of investigating pteropods in the size fractions > 63 µm instead of the > 125 µm only. In particular, neglecting the small size fraction may result in a remarkable (up to 50 %–60 %) underestimation of the relative abundance of the epipelagic species *Creseis acicula* and *Creseis conica* and the mesopelagic species *Heliconoides inflatus*. This may significantly affect palaeoenvironmental reconstructions. The observed presence of tropical species supports the suggestion that the eastern Mediterranean is a refugium for these species. This study provides a basic benchmark for the late Holocene evolution of pteropod and heteropod distribution over 5800–5300 cal BP across the base of the south-eastern Levantine margin.

## 1 Introduction

Holoplanktonic gastropods, representing less than 1 % of the total marine gastropod population, spend their entire life cycle in the water column (Wall-Palmer et al., 2014). They constitute an important part of the marine food web and have a major role in the carbon cycle, producing aragonite shells (Bè and Gilmer, 1977; Pierrot-Bults and Peijnenburg, 2015). The order Pteropoda, one of the major carbonate-producing holoplanktonic gastropods (Be and Gilmer, 1977; Van der Spoel, 1967; Janssen, 2012), includes three suborders: Euthecosomata, Pseudothecosomata, and Gymnosomata.

The Euthecosomata pteropods, which are the focus of this research, are divided into two superfamilies: Limacinoidea Gray, 1850 (trochospiral) and Cavolinioidea Gray 1850 (elongated or bilaterally symmetrical). The holoplanktonic gastropod group Heteropoda has been recently classified in the superfamily Pterotracheoidea within the order Littorinimorpha (Wall-Palmer et al., 2014). The holoplanktonic gastropod shells, made of aragonite, are dissolution susceptible and are more likely to be preserved in the fossil record in highly saline marginal seas, such as the Red Sea and the eastern Mediter-

anean Basin (Almogi-Labin and Reiss, 1977; Berner, 1977; Berger, 1978; Almogi-Labin et al., 2008). According to various studies, the recent Mediterranean pteropod fauna includes transitional, subtropical, and tropical species (Herman and Rosenberg, 1969; Biekart, 1989; Janssen et al., 2014; Wall-Palmer et al., 2014; Johnson et al., 2020). In particular the eastern Mediterranean is characterized by more tropical species, such as *Hyalocylis striata* (Rang, 1828) and *Cavolinia* spp. (e.g. Grecchi, 1984; Bogi and Galil, 2004; Janssen, 2012; Giamali et al., 2020). The decrease in pteropod species diversity in the Mediterranean from the west to the east and from the north to the south seems related to an increase in temperature and salinity and a decrease in nutrient content. Pteropoda assemblages have been described from all over the Mediterranean (Almogi-Labin and Reiss, 1977; Furnestin, 1979; Buccheri and Torelli, 1981; Corselli and Grecchi, 1987, 1990; Biekart, 1989; Violanti et al., 1991; Grecchi, 1994; Janssen, 2012).

Studies on living assemblages revealed the existence of two different groups based on migratory behaviours: the mesopelagic daily migratory and the epipelagic non-migratory pteropods (van der Spoel, 1967; Frontier, 1973; Bè and Gilmer, 1977; Wormuth, 1981; Almogi-Labin et al., 1988, 1991). Epipelagic organisms are usually restricted to the surface mixed layer in the Gulf of Aqaba, Red Sea, whereas mesopelagic migratory pteropods are controlled to a large degree by the oxygen levels in the intermediate waters (Red Sea; Almogi-Labin et al., 1984, 1991, 2008).

Pteropods were recently found to be well preserved in the deep water of the Levantine Basin (Hyams-Kaphzan et al., 2018).

The aim of this paper is to document the prevailing pteropod and heteropod assemblages across the base of the south-eastern margin of this basin, including the juvenile stages that comprise a large part of the assemblages, by using sediment cores retrieved during the EUROFLEETS2 SEMSEEP cruise in September 2016 (Makovsky et al., 2016).

## 2 Study area

The Mediterranean Sea is a semi-enclosed basin, characterized by an anti-estuarine thermohaline circulation (Ozer et al., 2020), with Atlantic surface water entering through the Strait of Gibraltar. These waters move eastwards and are modified to the saltier Levantine Surface Water (LSW) by evaporation in the easternmost part of the Mediterranean Sea (Malanotte-Rizzoli et al., 2014; Katz et al., 2020). The Levantine Basin has the saltiest and warmest waters of the entire Mediterranean Sea, with a sea surface salinity of up to 39.7‰ during summer and sea surface temperature ranging between  $\sim 16^\circ\text{C}$  in winter and  $30.8^\circ\text{C}$  in summer (Ozer et al., 2017). The thermohaline circulation and the formation of intermediate and deep water are important for marine ecosystems and biogeochemical cycles (Herut et al., 2000;

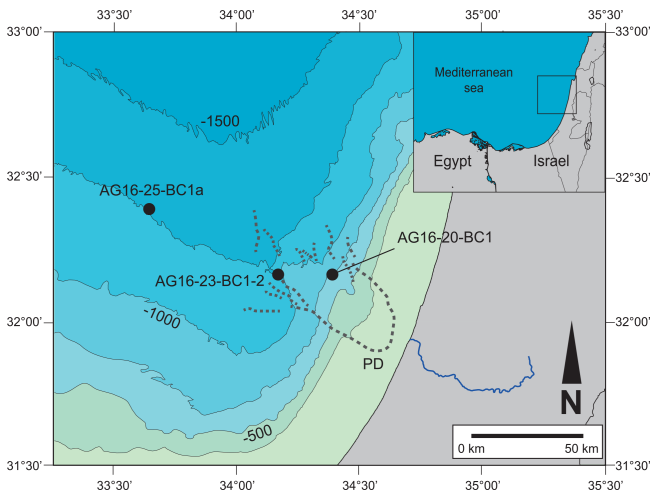
Janssen and Peijnenburg, 2014). Below the LSW lies the Levantine Intermediate Water (LIW) mass. Its formation occurs mainly in winter close to the Rhodes Gyre when the LSW cools down and sinks to intermediate water depths (Ozer et al., 2017, 2020) and through cascading events in shelf regions, contributing to the ventilation of the intermediate and deep waters (Waldman et al., 2018). The LIW mass flows westward, exiting the Mediterranean Sea via the Strait of Gibraltar carrying nutrients that impoverish the eastern Mediterranean waters (Herut et al., 2000; Gómez et al., 2000; Malanotte-Rizzoli et al., 2014).

The eastern Mediterranean Levantine Basin is currently an ultra-oligotrophic marine system. The Levantine Surface Water reaches a depth of 60–80 m with a surface temperature of  $28^\circ\text{C}$  and salinities varying between 39.2‰ and 39.3‰. Below this layer, a salinity below 38.8‰ represents the Modified Atlantic Water (MAW). In this water mass, temperature drops by  $10^\circ\text{C}$ , decreasing more slowly between 100–500 m depth and reaching minimum values of  $\sim 14^\circ\text{C}$ . In the underlying Levantine Intermediate Water (LIW), between 100 and 350 m water depth, the salinity and temperature slightly increase up to 39‰ and  $15^\circ\text{C}$ , respectively. Below the LIW, lies the eastern Mediterranean Deep Water mass (EMDW). Until the late 1980s, the EMDW originated only in the Adriatic Sea, with a relatively stable salinity and temperature of 38.7‰ and  $13.35^\circ\text{C}$ , respectively (Roether et al., 2007). Then, warmer temperature and more saline water from the Aegean Sea became a new source for the EMDW (e.g. Roether et al., 2007), moving westward through the Cretan Sea. Recent surveys documented colder and less saline water masses at the bottom of the basin, again derived from the Adriatic Sea province (Gertman et al., 2016; Ozer et al., 2020). All the sites included in this work are influenced by the EMDW.

The seafloor across much of the Levantine Basin comprises the eastern deep-sea fan of the Nile River, which is characterized by deep-sea channel systems (e.g. Gvirtzman et al., 2015). The Nile fan and the south-eastern Mediterranean continental margin, offshore of southern Israel, bounding it to the east are deformed due to the mobilization of the Messinian evaporites and overlying sediments. In particular, SEMSEEP surveying was focused on a large-scale ( $15 \times 50$  km), long-term salt-rooted rotational slide, the Palmahim Disturbance (PD), which is located across the southern portion of this margin (Garfunkel, 1979). On the northern margin of PD, between water depths of  $\sim 500$  to 800 m, deep-sea corals and associated habitats are settled on rocky authigenic carbonate outcrops that are associated with palaeo-seepage (Coleman et al., 2012; Spiro et al., 2021). At the western toe region of PD several active seepage features, including carbonate crusts, bacterial mats, bivalve beds, and chemosymbiotically living fauna, were documented in  $\sim 1$  km scale pockmarks (Coleman et al., 2012; Rubin-Blum et al., 2014; Basso et al., 2020; Beccari et al., 2020; Sisma-Ventura et al., 2022).

**Table 1.** Location, coordinates, and water depth of the studied cores. Northern Palmahim Disturbance coral site (AG16-20-BC1b), western Palmahim Disturbance pockmarks (AG16-23-BC2), and Gal-C channel area (AG16-25-BC1a).

Station	Location	Date	Latitude N	Longitude E	Water depth (m)	Distance from the Israeli coastline [km]
AG16-20-BC1	N Palm. Dist. coral site	26 September 2016	32°09.650′	34°23.700′	690	~ 40
AG16-23-BC2	W Palm. Dist. pockmarks	27 September 2016	32°09.650′	34°10.060′	1038	~ 60
AG16-25-BC1a	Gal-C channel area	28 September 2016	32°24.010′	33°39.450′	1310	~ 100

**Figure 1.** Location map of the studied area. The three studied locations are illustrated: AG16-20-BC1b, coral area (WA5, 690 m depth); AG16-23-BC2, pockmark area (WA3, 1038 m depth); AG16-25-BC1a, Gal-C channel area (WA2c, 1310 m depth). Map created and modified from Generic Mapping Tools (GMT 5; Wesel et al., 2013).

### 3 Material and methods

#### 3.1 Sample preparation

Samples were collected along the Israeli coast during the EUROFLEETS2 SEMSEEP cruise on board R/V *Aegaeo* in September 2016 (Makovsky et al., 2016; our Fig. 1, Table 1). A box corer with a sampling area of 30 × 30 cm and 60 cm penetration depth was used to retrieve undisturbed samples. Several cores were sub-sampled for different purposes (e.g. micropalaeontology, sedimentology, geochemistry). The sub-cores selected for micropalaeontology have an inner diameter of 9 cm and were sliced on board at 1 cm resolution.

Sediments are predominantly brownish pelagic clay, often intercalated with light and/or dark lenses. Surface sediments show slight (AG16-25-BC1a) to intense (AG16-23-BC1) bioturbations (Makowski et al., 2017). In core AG16-20-BC1b, collected in the region characterized at present

by cold-water corals, washed residues also contain elements from a seep environment, e.g. black and orange tubes, and gypsum crystals. This environment will therefore be informally denominated as the “coral-transition core” or “coral-transition area”.

Samples were studied at 2 cm intervals. Bulk sediments were air-dried, weighed, and placed in a graded beaker, where afterward a known volume of water was added; then the sample volume was estimated. Bulk sediments were then washed with a 32 µm mesh sieve and air-dried, and the residues were weighed. Grain size analyses were performed by dry sieving the residues using sieves with different mesh sizes (> 500, 250–500, 125–250, 63–125, 32–63, and < 32 µm), and each obtained fraction was weighed.

Stable isotopes analyses on *Globigerinoides ruber* (d’Orbigny, 1835) (5–10 specimens) were done on the size fraction 125–250 µm. Stable isotope measurements were carried out at the Stable Isotope Laboratory at UiT (The Arctic University of Norway). Samples were placed in 4.5 mL vials, flushed with He and H<sub>3</sub>PO<sub>4</sub>, equilibrated for more than 2 h at 50 °C, and then analysed on a Gasbench II and MAT253 IRMS for δ<sup>18</sup>O. Results were normalized to VPDB. A standard deviation of ≤ 0.1 ‰ expresses the long-term instrumental accuracy (ThermoScientific).

Specimens for isotope analyses were picked from the size fraction > 250 µm and cleaned in an ultrasound bath for a few seconds to remove any possible contaminations. Since in some samples both benthic and planktonic foraminifera were rare, the picking interval was extended to include two to three samples to reach at least 4–12 mg of pure carbonate.

Rock-Eval analyses were performed on sediments using a standard Rock-Eval 6 (Technologies Vinci, Rueil-Malmaison, France) at the University of Lausanne. The technique involves pyrolysis in an inert atmosphere followed by oxidation, with temperatures of between 200–850 °C. This methodology was used for determining the total organic carbon (TOC in wt %) and carbonate (wt %) content in the studied samples; its accuracy, evaluated to less than 2.5 wt %, is extensively described in Behar and Beaumont (2001).

### 3.2 Pteropoda identification and Heteropoda checklist

#### 3.2.1 Pteropoda

Residue fractions were split into aliquots containing about 300 pteropod shells using a 1/8 Simpson microsampler with a slot width of 500  $\mu\text{m}$ . Attention was paid to ensuring that pteropods did not become entangled in the splitter slots. A total of about 900 specimens was counted in three sediment fractions (> 250, 125–250, and 63–125  $\mu\text{m}$ ) to evaluate the abundance of both juveniles and adult specimens. The results were referenced to 1 g of sediments. Only whole specimens or fragments with preserved protoconchs were counted to avoid possible miscounting following, e.g., Wall-Palmer et al. (2014).

In some cases, the identification of pteropods, especially of their juvenile stage, was difficult. In particular, the distinction between the juveniles of *Cavolinia gibbosa* (d'Orbigny, 1835) and *Cavolinia inflexa* (Lesueur, 1813) was uncertain. For this reason, these species were grouped into *Cavolinia* spp. Furthermore, due to difficulties in identifying the juvenile stages of *Creseis acicula* (Rang, 1828) and *Creseis conica* Eschscholtz, 1829, they were lumped together and presented as *Creseis* spp. Additional holoplanktonic molluscs are very rare in the samples, and their ecological significance is poorly known; therefore only a checklist is given. They include *Clionidarum* sp. 1 and *Clionidarum* sp. 2, species belonging to the Gymnosomata (as defined by Janssen et al., 2012), and the Pseudothecosomata *Gleba cordata* Forsskål in Niebuhr, 1776 and *Pterotracheoidea* spp. Species richness and Shannon index ( $H'$ ) were calculated on log-transformed data referenced to 1 g of sediment using the software Primer v7 (Clarke and Gorley, 2015). Pteropod species are listed in Table 2 and illustrated in Figs. 2–3.

#### 3.2.2 Heteropoda

The best preserved specimens of adults and juveniles heteropods were picked from the fractions > 250 and 125–250  $\mu\text{m}$  to compile a checklist of species present in the Levantine Basin (Table 2, Fig. 4). Specimens in the size fraction > 250  $\mu\text{m}$  were counted for comparison with pteropods. Heteropods are generally identified by the size of the shell, the size of the keel and its ornamentations, and the size, shape, and ornamentation of the larval stage (Wall-Palmer et al., 2020). However, the identification of some species of the genus *Atlanta* is based on the eye type, radula, and operculum, elements that are not preserved in the fossil record. For this reason, although known for 200 years they have been generally overlooked in palaeoceanographic studies, and, therefore, their ecological preferences are not sufficiently known (e.g. Wall-Palmer et al., 2016).

### 3.3 Radiocarbon dating

For core AG16-20-BC1b the benthic foraminifer *Cibicides pachyderma* (Rzehak, 1886) was selected as it was one of the most abundant and massive species, whereas for cores AG16-23-BC2 and AG16-25-BC1a the planktonic foraminifera *G. ruber* and *Trilobatus sacculifer* (Brady, 1877) were used. The required 0.5 to 1 mg of carbon was retrieved from ca. 4–8 mg of shell (pure calcite). These were placed in the gas bench vials, flushed with a helium stream, and dissolved in concentrated phosphoric acid (85 %) (Molnar et al., 2013). The  $\text{CO}_2$  was carried to the graphitization line and reduced to graphite (Nemec et al., 2010). The graphite samples were pressed into the aluminium cathodes and measured using the dedicated AMS  $^{14}\text{C}$  system (MICADAS) at ETH Zurich (Synal et al., 2007). The results were calibrated using the OxCal 4.4 online software (Ramsey, 2021) and the Marine20 calibration curve (Heaton et al., 2020) with a local reservoir age correction of  $\Delta R = -94 \pm 94$ .

## 4 Results

Thirteen species of pteropods and seven species of heteropods are identified in the studied cores (Table 2; Supplement S1). The assemblages are mainly composed of the species *C. acicula*, *C. conica*, *H. striata*, *Limacina trochiformis* (d'Orbigny, 1835), *Heliconoides inflatus* (d'Orbigny, 1835), *Peracle reticulata* (d'Orbigny, 1835), *Styliola subula* (Quoy and Gaimard, 1827), and *Clio pyramidata* (Linnaeus, 1767). Some of these species have an epipelagic life strategy (*Cavolinia* spp., *C. acicula*, *C. conica*, *H. striata*, *L. trochiformis*), and some are mesopelagic species (*C. pyramidata*, *Clio cuspidata*, *H. inflatus*, *Limacina bulimoides*, *P. reticulata*, *S. subula*).

In all samples, *Creseis* spp. and related protoconchs are the most abundant species, reaching up to 96 % of the total number of pteropods collected in the > 63  $\mu\text{m}$  sediment fraction. However, the two species *C. acicula* and *C. conica* were identified only in the coarser fractions (> 250 and 125–250  $\mu\text{m}$ ).

Pteropod specimens show different states of shell preservation varying between well-preserved transparent shell to internal moulds. Also, distinct differences in abundance of these species have been observed with distinctly higher abundances in the fraction > 63  $\mu\text{m}$  compared to the > 125  $\mu\text{m}$  fraction (Fig. 5a–k).

Epipelagic species clearly dominate the assemblage in the > 63  $\mu\text{m}$  fraction in the three cores (Table 2) reaching, respectively, 96 % in core AG16-20-BC1b (Fig. 5Ab), 82 % in core AG16-23-BC2 (Fig. 5Bb), and 86 % in core AG16-25-BC1a (Fig. 5Cb). The most common epipelagic species in the three cores are *Creseis* spp. and *L. trochiformis*. In the > 125  $\mu\text{m}$  fraction, the relative abundance of the mesopelagic species increases significantly up to 77 % of the assemblage in core AG16-20-BC1b (up to 37 % in the > 63  $\mu\text{m}$  fraction),



**Figure 2.** Pteropoda from the Levantine Basin (offshore of Israel). (1)–(5) *Limacina trochiformis* (d’Orbigny, 1835), from juvenile to adult specimen; (6)–(10) *Limacina bulimoides* (d’Orbigny, 1835), from juvenile to adult specimen; (11)–(12) *Heliconoides inflatus* (d’Orbigny, 1835), adult specimens, (11) spiral view, (12) aperture view; (13) *Creseis conica* (Eschscholtz, 1829); (14) *Creseis acicula* (Rang, 1828); (15)–(16) *Cavolinia gibbosa* (d’Orbigny, 1835), adult specimens, (15) side view, (16) ventral view; (17)–(18) *Cavolinia inflata*, adult specimens, (17) side view and (18) dorsal view; (19)–(20) *Cavolinia* spp. protoconch, (19) side view and (20) dorsal view.

63 % in core AG16-23-BC2 (up to 33 % in the  $> 63 \mu\text{m}$  fraction), and 75 % in core AG16-25-BC1a (up to 45 % in the  $> 63 \mu\text{m}$  fraction). The most common mesopelagic species in the cores are *H. inflatus*, *L. bulimoides*, and *S. subula*.

Seven heteropod species are recognized in the fraction  $> 250 \mu\text{m}$ , as reported in Table 2, but they mostly consist of juvenile specimens. Since the morphology of the shell is not sufficient to identify all specimens at species level, only the following species of heteropods were identified: *Atlanta helicinoidea* (Gray, 1850), *Atlanta selvagensis* (de Vera and

Seapy, 2006), *Protatlanta souleyeti* (Smith, 1888), *Atlanta rosea* (Gray, 1850), *Oxygyrus inflatus* (Benson, 1835), *Atlanta turriculata* (d’Orbigny, 1835), and *Firoloida desmarestia* (Lesueur, 1817).

#### 4.1 Core results

##### 4.1.1 Coral-transition area (core AG16-20-BC1b)

In core AG16-20-BC1b, 12 pteropod species were identified, ranging from 49 to 600 individuals  $\text{g}^{-1}$  (ind  $\text{g}^{-1}$ ) in the

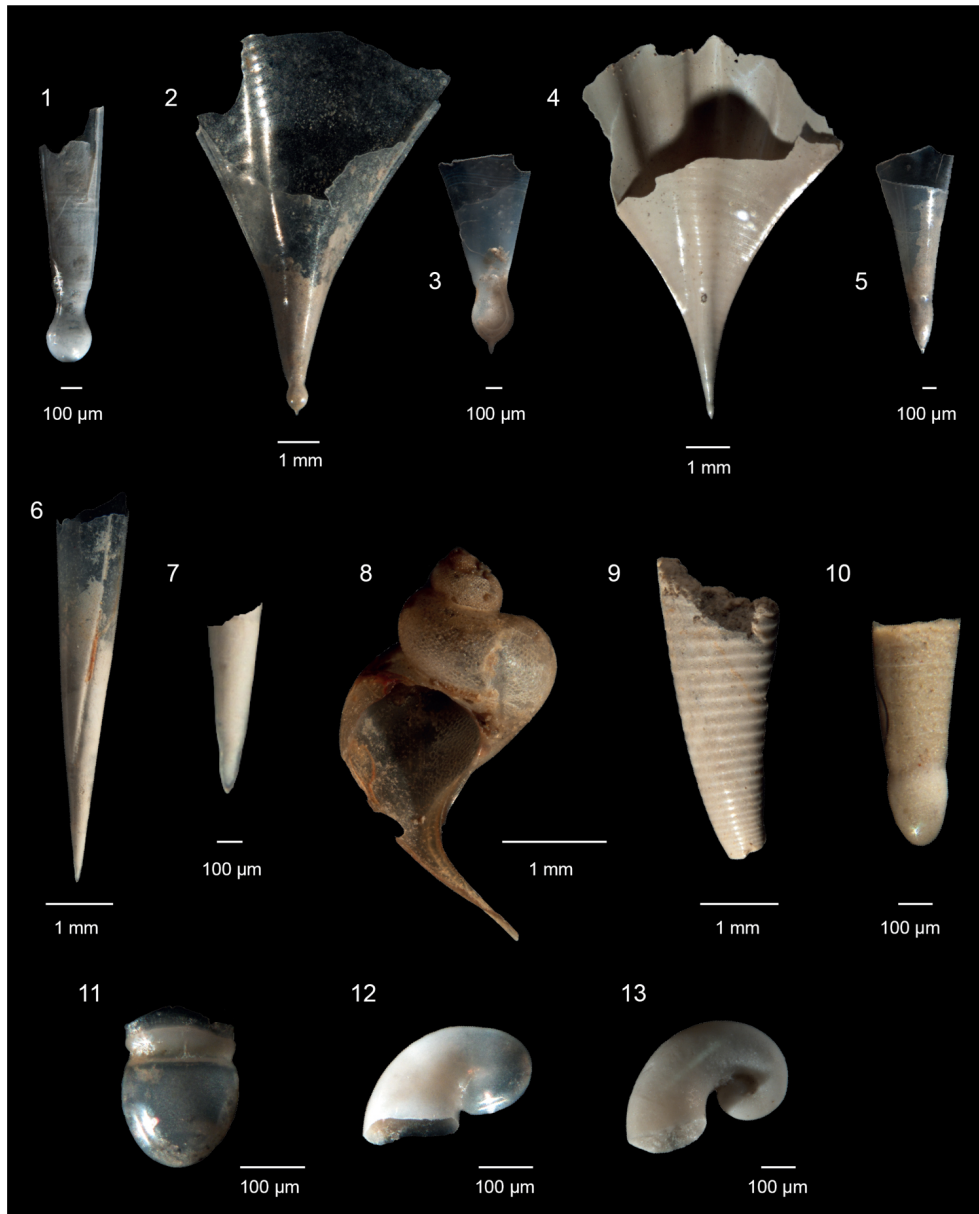


**Figure 3.** Pteropoda from the Levantine Basin (offshore of Israel). (1) *Diacria trispinosa* (de Blainville, 1821) protoconch; (2)–(3) *Clio cuspidata* (Bosc, 1801), (2) adult specimen, (3) protoconch; (4)–(5) *Clio pyramidata* (Linnaeus, 1767), (4) adult specimen, (5) protoconch; (6)–(7) *Styliola subula* (Quoy and Gaimard, 1827), (6) adult specimen, (7) protoconch; (8) *Peracle reticulata* (d’Orbigny, 1835); (9) *Hyalocylis striata* (Rang, 1828); (10) *Clionidarum* sp. 2; (11) *Clionidarum* sp. 1; (12) *Gleba cordata* (Niebuhr, 1776); (13) Pterotrachea sp.

> 63 µm fraction with maximum abundance in the lower part of the core at 28–29 cm depth (Fig. 5Ad). The most abundant taxon is *Creseis* spp., reaching up to 96 % of the assemblage in the lower part of the core (Fig. 5Ae). Also abundant is *H. inflatus*, reaching up to 35 % of the assemblage. *Heliconoides inflatus* does not occur in the middle part of the core and at 12–13 cm depth in the grain size fraction > 250 µm, although it occurs only in the finer size fractions. Rarer and mainly present in the upper part of the core are *L. bulimoides* (up to 14 %), *L. trochiformis* (up to 6 %), and *S. subula* (up to 5 %)

The Shannon index varies along the core with a maximum value occurring at 8–9 cm ( $H' = 1.5$ ; Fig. 5Ac).

Pteropod abundances range from 6 to 63 ind g<sup>-1</sup> in the > 125 µm fraction (Fig. 5Ah). The most common species are *Creseis* spp. and *H. inflatus* in the > 63 µm fraction with *Creseis* spp. decreasing down to 62 % and *H. inflatus* increasing up to 72 % (Fig. 5Ai, j). Remarkable relative abundance values of *S. subula* occur in the upper part of this core (up to 18 %). The species occurring in the > 63 µm fraction are present in considerable numbers also in the 125 µm frac-



**Figure 4.** Heteropoda from the Levantine Basin (offshore of Israel). (1)–(4) *Atlanta selvagensis* (de Vera and Seapy, 2006), (1)–(2) juvenile specimens, (1) aperture view, (2) spiral view; (3)–(4) adult specimens, (3) aperture view, (4) spiral view; (5)–(6) *Atlanta helicinoidea* (Gray, 1850), (5) aperture view, (6) spiral view; (7)–(10) *Protatlanta souleyeti* (Smith, 1888), (7)–(8) juvenile specimens, (7) aperture view, (8) spiral view; (9)–(10) adult specimens, (9) aperture view, (10) spiral view; (11)–(12) *Atlanta rosea* (Gray, 1850), (11) aperture view, (12) spiral view; (13)–(16) *Atlanta turriculata* (d’Orbigny, 1835), (13)–(14) juvenile specimens, (13) aperture view, (14) spiral view, (15)–(16) adult specimens, (15) aperture view, (16) spiral view; (17)–(18) *Oxygyrus inflatus* (Benson, 1835), (17) aperture view, (18) spiral view; (19)–(20) *Firoloidea desmarestia* (Lesueur, 1817), (19) aperture view, (20) spiral view.

tion. In particular, the relative abundance of *L. bulimoides* increases up to 22% and *L. trochiformis* up to 16%. Few specimens of *D. trispinosa* are present at 18–19 cm, comprising up to 4%, and *C. pyramidata* at 6–7 cm comprises up to 4% of the assemblage.

In the > 250 µm fraction the pteropods and heteropods follow a similar distribution pattern downcore to a depth of 23 cm, with heteropods always being less abundant than the pteropods (Fig. 5Ak).

The sediments consist of mud, the sand fraction comprising less than 5% of the total sediment weight (Fig. 6a). Small fragments of carbonate crusts or large pteropod or heteropod

shells are not observed in this core. The  $\delta^{18}\text{O}$  ranges from  $-0.22\text{‰}$  to  $-0.52\text{‰}$  at the top and base of the core, respectively, with a maximum negative value of  $-1.28\text{‰}$  at 20–21 cm. The TOC wt% values vary from 0.34 to 1.15, with the highest value of 1.15 wt% occurring at 26–27 cm (Fig. 6a). Carbonate content varies from 7.8 wt% to 21.8 wt% with higher values occurring from around 18 cm and continuing downcore (Fig. 6a).

Radiocarbon dating gives an age of 1122–680 cal BP for the upper part of the core, 2820 to 2317 cal BP (1430 ± 20 BP, 2876 ± 21 BP) for the middle part, and 3542

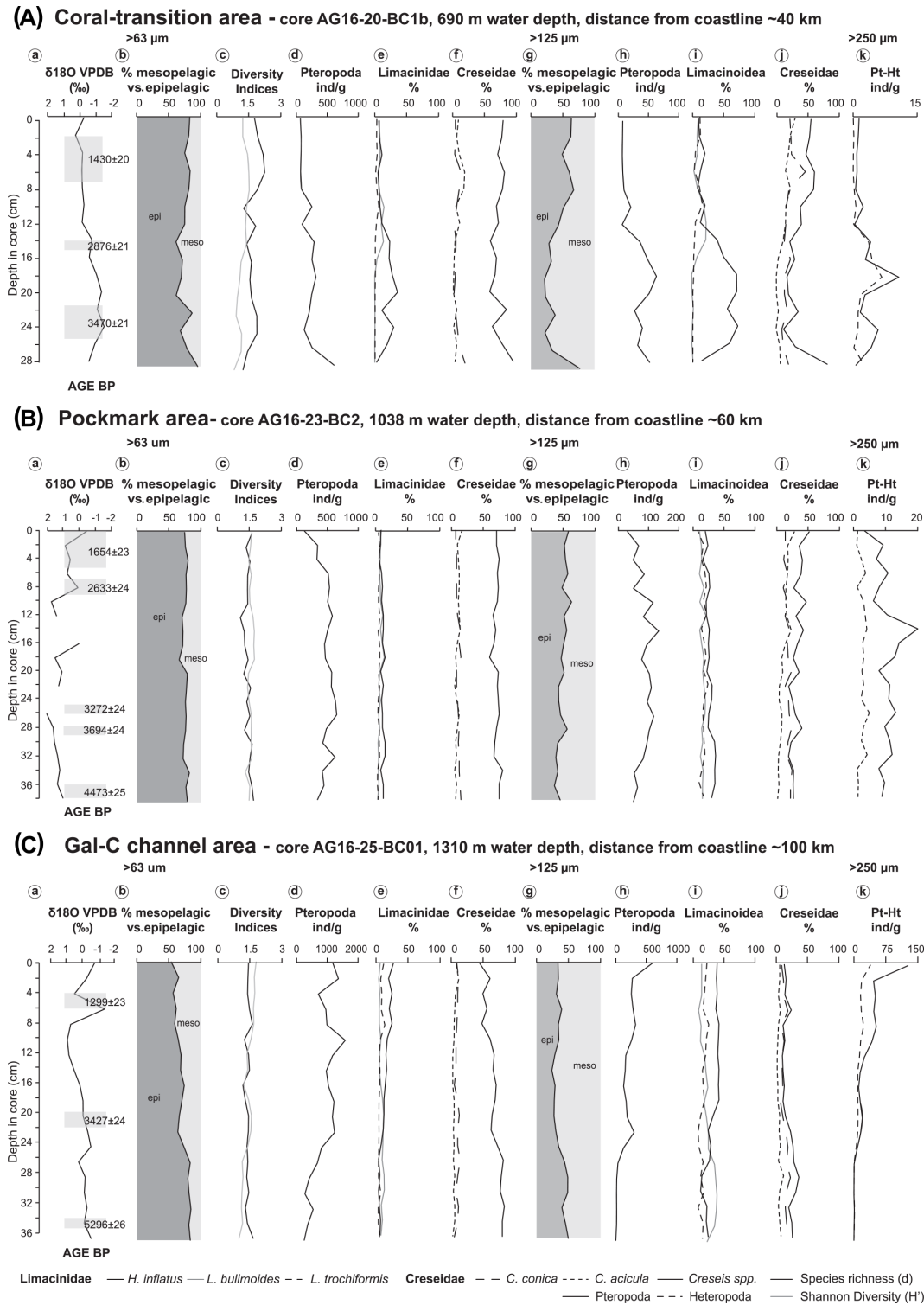


**Figure 5.** Stable isotopes, dating, and quantitative analyses of pteropods (b–f for the > 63 μm and g–j for the > 125 μm size fraction) for the following cores: **(A)** coral-transition area (core AG16-20-BC1b), **(B)** pockmark area (core AG16-23-BC2), and **(C)** Gal-C channel area (core AG16-25-BC1a). (a) δ<sup>18</sup>O values and radiocarbon dating (<sup>14</sup>C) shown for each core. (b, g) % epipelagic (dark grey) vs. % mesopelagic (light grey) species; (c) species richness (solid black line) and Shannon diversity (H', solid light grey line), calculated on the total fraction > 63 μm. (d, h) Pteropod abundance per gram of sediment; (e, i) Limacinioidea: percentage of *H. inflatus* (solid line), *L. bulimoides* (grey solid line), and *L. trochiformis* (dashed line). (f, j) Creseidae: percentage of *C. conica* (widely spaced dashed line), *C. acicula* (closely spaced line), and unidentified protoconchs of *Creseis* spp. (solid line). (k) Numerical abundance per gram of pteropods vs. heteropods in the > 250 μm fraction.

**Table 2.** Minimum and maximum abundances of pteropods and heteropods for each sample in the investigated cores. The number of pteropods per gram of sediment is reported in Supplement S1. X: presence of species or genera that have not been counted.

Species		AG16-20-BC1b no. per sample (min–max)	AG16-23-BC2 no. per sample (min–max)	AG16-25-BC01 no. per sample (min–max)
Pteropoda, Euthecosomata				
<i>Heliconoides inflatus</i> (d’Orbigny, 1835)	Mesopelagic	77–2313	96–1216	230–7173
<i>Limacina bulimoides</i> (d’Orbigny, 1835)	Mesopelagic	1–1345	126–1239	370–2800
<i>Limacina trochiformis</i> (d’Orbigny, 1835)	Epipelagic	0–135	59–683	185–2667
<i>Creseis acicula</i> (Rang, 1828)	Epipelagic	8–593	139–915	89–2130
<i>Creseis conica</i> (Eschscholtz, 1829)	Epipelagic	65–2476	63–1088	320–3144
<i>Creseis</i> spp.	Epipelagic	801–8596	571–4172	1832–19 704
<i>Styliola subula</i> (Quoy and Gaimard, 1827)	Mesopelagic	9–158	12–114	0–3431
<i>Cavolinia gibbosa</i> (d’Orbigny, 1835)	Epipelagic			
<i>Cavolinia inflexa</i> (Lesueur, 1813)	Epipelagic			
<i>Cavolinia</i> spp.	Epipelagic	0–150	0–23	2–35
<i>Diacria trispinosa</i> (de Blainville, 1821)	Mesopelagic	0–67	0–8	0–8
<i>Clio pyramidata</i> (Linnaeus, 1767)	Mesopelagic	0–42	16–336	8–113
<i>Clio cuspidata</i> (Bosc, 1801)	Mesopelagic	0–12	0–8	0–12
<i>Hyalocylis striata</i> (Rang, 1828)	Epipelagic	0–12		0–1
<i>Peracle reticulata</i> (d’Orbigny, 1835)	Mesopelagic		0–1	0–46
Gymnosomata				
<i>Clionidarum</i> sp. 1		X	X	X
<i>Clionidarum</i> sp. 2				X
<i>Gleba cordata</i>		X	X	X
<i>Pterotrachea</i> sp.		X	X	X
Heteropoda				
<i>Atlanta selvagensis</i> (de Vera and Seapy, 2006)		X	X	X
<i>Atlanta rosea</i> Gray, 1850		X	X	X
<i>Atlanta helicinoidea</i> (Gray, 1850)				X
<i>Atlanta turriculata</i> d’Orbigny, 1835		X	X	X
<i>Oxygyrus inflatus</i> Benson, 1835		X	X	X
<i>Firoloida desmarestia</i> Lesueur, 1817		X	X	X
<i>Protatlanta souleyeti</i> (Smith, 1888)		X	X	X

to 3024 cal BP ( $3470 \pm 21$  BP) for its lower part (Fig. 5A; Table 3).

#### 4.1.2 Pockmark area (core AG16-23-BC2)

In core AG16-23-BC2, 13 pteropod species are identified, ranging from 134 to  $655 \text{ ind g}^{-1}$  in the  $> 63 \mu\text{m}$  fraction (Fig. 5Bd). *Creseis* spp. is the most common taxon, reaching up to 79 % of the assemblage (Fig. 5Bf). *H. inflatus* is also abundant, reaching up to 16 % of the assemblage, co-occurring with *L. bulimoides* (up to 15 %), *L. trochiformis* (up to 7 %), *S. subula* (up to 4 %), and *C. pyramidata* (4 %) (Fig. 5Be). The Shannon index reaches the maximum value at 12–13 cm ( $H' = 1.7$ ; Fig. 5Bc).

In the  $> 125 \mu\text{m}$  fraction, pteropods range in abundance from 33 to  $13 \text{ ind g}^{-1}$  (Fig. 5Bh). The most common species are *Creseis* spp., reaching a relative abundance of up to 52 %

of the assemblage composition (Fig. 5Bj). *H. inflatus* comprises up to 35 %, *L. bulimoides* up to 18 %, *L. trochiformis* up to 23 %, *S. subula* up to 11 %, and *C. pyramidata* up to 14 % (Fig. 5Bi). In the  $> 250 \mu\text{m}$  fraction, pteropods and heteropods follow the same distribution pattern along the whole core, although pteropods are more abundant (Fig. 5Bk).

Sand content in this core is below 13 % (Fig. 6b). Small fragments of carbonate crusts and shrimp claws are present only in the lower part of this core. The  $\delta^{18}\text{O}$  ranges from  $-0.44 \text{ ‰}$  to  $1.02 \text{ ‰}$  at the top and base of the core, respectively, with a more positive value of  $2.04 \text{ ‰}$  at 26–27 cm. The highest sand percentage is  $\sim 13 \text{ ‰}$  at 34–35 cm (Fig. 6). Carbonate content is below 20 % at the core top increasing towards the core bottom (Fig. 6b). Total organic carbon content varies from 0.24 % to 0.61 %, being the highest at the core top (Fig. 6b).

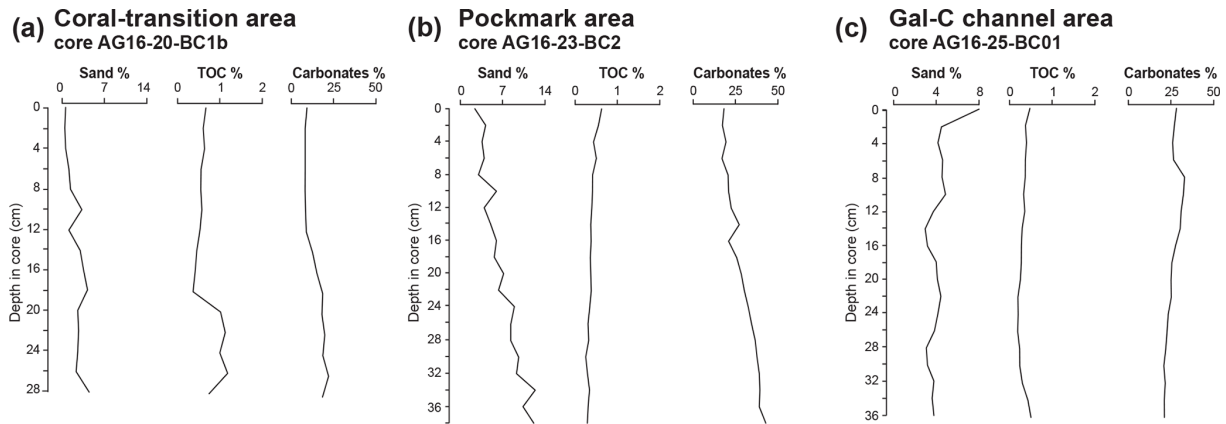


**Figure 6.** Sand content in the  $> 63 \mu\text{m}$  fraction, total organic carbon (TOC %), and carbonates (%) in the three studied areas: the (a) coral-transition area, the (b) pockmark area, and the (c) Gal-C channel area.

The age, based on planktonic foraminifera, is between 1347–917 and 4836–4293 cal BP ( $1654 \pm 23$  BP at 0–5 cm;  $2633 \pm 24$  BP at 6–9 cm;  $3694 \pm 24$  BP at 27 cm; and  $4473 \pm 25$  BP at 37 cm) (Fig. 5B).

#### 4.1.3 Gal-C channel area (core AG16-25-BC1a)

In core AG16-25-BC1a, 13 pteropod species range from 368 to  $1618 \text{ ind g}^{-1}$  in the  $> 63 \mu\text{m}$  fraction (Fig. 5Cd). The most abundant genus is *Creseis* spp., reaching up to 82 % of the assemblage. The number of *Creseis* spp. slightly decreases upcore (Fig. 5Cf), and *H. inflatus* increases upward, reaching a maximum of 28 % at the core top (Fig. 5Ce). Other species are less abundant such as *L. bulimoides* (up to 12 %), *L. trochiformis* (up to 13 %), and *S. subula* (up to 10 %). The Shannon index reaches the maximum value at the surface ( $H' = 1.8$ ; Fig. 5Cc).

Pteropod abundances range from 12 to  $589 \text{ ind g}^{-1}$  in the  $> 125 \mu\text{m}$  fraction (Fig. 5Ch). The most common species include *H. inflatus*, which reaches abundances of up to 41 %; *Limacina bulimoides* reaches abundances of up to 34 %, *L. trochiformis* of up to 24 %, and *Creseis* spp. of up to 37 % (Figs. 5Ci, Cj). Significant relative abundances of *S. subula* (up to 21 %) are observed from the top of this core down to 25 cm. A few specimens of *C. pyramidata* are also present comprising up to 5 % of the total assemblage. Adult specimens of heteropods co-occurring with juveniles are observed only in this core, in particular the species *A. selvagensis* (Fig. 5Ck).

In the  $> 250 \mu\text{m}$  fraction, the number of pteropods and heteropods is similar in the lower part of the core down to 26–27 cm, whereas pteropods are more abundant upward, but the two curves follow the same trend (Fig. 5Ck).

Fine sandy sediments (up to 8 % at 0–1 cm) characterize the core top (Fig. 6c). This higher abundance of the sandy fraction is due to the presence of large pteropods and het-

eropods. Below 0–1 cm, the sand content varies between 3 % and 4 %.

The  $\delta^{18}\text{O}$  ranges from  $-0.73\text{‰}$  to  $-0.52\text{‰}$  at the top and base of the core, respectively, with a maximum negative value of  $-1.37\text{‰}$  at 6–7 cm.

The TOC wt % content is low, varying between 0.20 % and 0.51 % throughout the core (Fig. 6c). Carbonate wt % content varies from 21 to a maximum value of 33 % at 8–9 cm depth in the core (Fig. 6c). This core represents the longest time record among the three studied cores with a basal age of  $5296 \pm 26$  BP at 35 cm depth (Fig. 5C, Table 3).

## 5 Discussion

Sand and carbonate percentage abundances displaying a similar trend in the three cores roughly reflect the depositional environments (Fig. 6). In particular, the highest sand and carbonate content is observed in the pockmark area, where it decreases in abundance from the bottom to the top of core AG16-23-BC2 due to the presence of seep-related carbonate crusts and shrimp claws in addition to the pelagic carbonate. These elements are missing or very rare in the Gal-C channel and in the coral area, where the carbonate content is mostly due to abundant pteropods and heteropods.

Pteropod shells have a high sinking velocity due to their mass, and their deposition occurs just below the organism's living habitats (Vinogradov, 1961), showing a clear similarity between living and dead assemblages in surface sediments (e.g. Almogi-Labin, 1984; Weikert, 1987). Of the 17 species described for the eastern Mediterranean Sea (Janssen, 2012), 13 are observed in this study. Diversity and specimen abundances in both the  $> 63$  and  $> 125 \mu\text{m}$  fractions is generally lower in the shallowest coral-transition area (690 m water depth and around 40 km distance from the coast) than in the deepest Gal-C channel area (1310 m water depth and around 100 km from the coast; Fig. 5Ac, Bc). A similar increase in pteropod abundances with increasing water depth has been

**Table 3.** Radiocarbon AMS14C of benthic (Bf; *Cibicidoides pachyderma*) and planktonic (Pf; *Globigerinoides ruber* and *Trilobatus sacculifer*) foraminifera obtained from cores AG16-20-BC1b, AG16-23-BC2, and AG16-25-BC1a. The three cores were dated independently: one was dated with benthic foraminifera and two were dated with planktonic foraminifera in the absence of sufficient benthic specimens for dating in all the three cores. The ages of benthic and planktonic foraminifera that were selected from the top layers of cores AG16-20-BC1b (2–7 cm; benthic foraminifera) and AG16-23-BC2 (0–5 cm; planktonic foraminifera) appear to be close (ca. 200 <sup>14</sup>C years difference). The benthic age is even younger, pointing to variability in the reservoir age of the mixed layer. The location of the sampling sites (close to the shore) might be the reason for such close reservoir ages between benthic and planktonic foraminifera. More details are reported in Supplement S1.

Core	Core depth	Material (cm)	Sample ID	<sup>14</sup> C age (yr BP)	1σ error (± years)
AG16-20-BC1b	2–7	Bf, <i>Cibicidoides pachyderma</i>	ETH-115056	1430	20
AG16-20-BC1b	14–15	Bf, <i>Cibicidoides pachyderma</i>	ETH-115057	2876	20
AG16-20-BC1b	22–25	Bf, <i>Cibicidoides pachyderma</i>	ETH-115058	3470	21
AG16-23-BC2	0–5	Pf, <i>G. ruber</i> and <i>T.sacculifer</i>	ETH-117606	1654	23
AG16-23-BC2	6–9	Pf, <i>G. ruber</i> and <i>T.sacculifer</i>	ETH-117607	2633	24
AG16-23-BC2	26–27	Pf, <i>G. ruber</i> and <i>T.sacculifer</i>	ETH-117608	3272	24
AG16-23-BC2	28–29	Pf, <i>G. ruber</i> and <i>T.sacculifer</i>	ETH-117609	3694	24
AG16-23-BC2	36–37	Pf, <i>G. ruber</i> and <i>T.sacculifer</i>	ETH-117610	4473	25
AG16-25-BC1a	4–5	Pf, <i>G. ruber</i> and <i>T.sacculifer</i>	ETH-117611	1299	23
AG16-25-BC1a	20–21	Pf, <i>G. ruber</i> and <i>T.sacculifer</i>	ETH-117612	3427	24
= AG16-25-BC1a	34–35	Pf, <i>G. ruber</i> and <i>T.sacculifer</i>	ETH-117613	5296	26

reported also by Cita and Zocchi (1978) and Hyams-Kaphzan et al. (2018). This suggests a different level of oceanographic interaction between the shelf and the continental slope, in agreement with the observations of Alkalay et al. (2020).

The best preservation of specimens observed in the deepest Gal-C channel area supports the idea that the eastern Mediterranean and the Red Sea act as a carbonate trap in the absence of an aragonite compensation depth (ACD) in water depths shallower than 3000 m (Berger, 1979).

In our study, we also report the presence of abundant protoconchs that cannot be identified at species level, although they are not strongly corroded. In particular, *Cavolinia* spp. protoconchs still present the very delicate thin narrow and parallel striations, which characterize them through their embryonic parts (Janssen et al., 2012), as also described by Almogi-Labin and Reiss (1977) for specimens collected in the Red Sea and the Gulf of Aqaba. Rare protoconchs of *Diacria trispinosa* (de Blainville, 1821) also occur in the studied areas as previously documented by Almogi-Labin and Reiss (1977). Their presence indicates that environmental conditions support the reproduction of these pteropod species.

### 5.1 Autoecology of pteropods and palaeoenvironmental interpretation

Planktonic gastropods, in particular pteropods, have been widely used for palaeoclimatic and palaeoceanographic reconstructions. They are very sensitive to the temperature and salinity of the water masses, which act as effective barriers

to the pteropod populations (e.g. Biekart, 1989; Thiede and Junger, 1992).

The observed *Heliconoides inflatus* is a mesopelagic, subtropical species living at a depth ranging from 200 to 1000 m, water temperatures of between 14 and 28 °C (Violanti et al., 1991; Grecchi, 1984; Van der Spoel, 1967), and salinity oscillations of between 36‰–41‰ in the Gulf of Aqaba (Bé and Gilmer, 1977; Almogi-Labin, 1982; Almogi-Labin, 1984). The epipelagic species *L. trochiformis* is considered to be a tropical species preferring water temperatures between 13.8–28 °C and salinities similar to *H. inflatus* (Almogi-Labin, 1982).

The genera *Creseis* and *H. inflatus*, observed as abundant in this study, have been argued by Almogi-Labin and Reiss (1977) and Violanti et al. (1991) to be dominant in the eastern Mediterranean Sea and present since the end of the last glaciation (Blanc-Vernet et al., 1969; Grecchi, 1984). Recent studies demonstrate that the mesopelagic *H. inflatus* and the epipelagic *Creseis* spp. are highly depth sensitive (e.g. Singh et al., 2001). Grecchi and Bertolotti (1988) point out that *G. cordata* (Pseudothecosomata), *Clionidarum* spp., and heteropods typically prefer warm waters. Wall Palmer et al. (2004) report that the heteropods *A. rosea* and *A. selvagensis* are typically found in tropical and subtropical water masses of the Atlantic Ocean.

Our results are consistent with the suggestion of Biekart (1989) that the easternmost part of the Levantine Basin acts as a refugium for warm-water pteropod species. *Cavolinia* is a warm-water genus, living between 0–250 m water depth, which has been documented as rare in the Lev-

antine Basin (Bè and Gilmer, 1977; Herman, 1981; Violanti et al., 1991; Janssen, 2012, and references therein). The geographical distribution of the *C. gibbosa* d'Orbigny 1835 subspecies *gibbosa* in the Levantine Sea has been used to suggest that this species could be a Tethyan relict, which survived the glacial cycles in this region (Rampal, 1980; Corselli and Grecchi, 1987; Biekart, 1989).

Therefore, the primary pteropod assemblages observed across the base of the south-eastern Mediterranean margin reflect a subtropical to temperate environment as also indicated by the  $\delta^{18}\text{O}$  values that are typical of the eastern Mediterranean region (Fig. 5Aa, and Ba; e.g. Hennekam et al., 2015; Mojathid et al., 2015). The only exceptions are the  $\delta^{18}\text{O}$  values measured from the specimens in the pockmark area (Fig. 5Ba). However, the isotopic signature of foraminiferal shell from these sediments might be affected by diagenesis due to biogeochemical processes resulting from methane emissions. As previously demonstrated by Dessandier et al. (2020), discrete authigenic calcite overgrowth on foraminifera altered their  $\delta^{18}\text{O}$  signature, corroborating the presence of seep-related features throughout the pockmark core.

The upper water masses of the Levantine Basin are characterized by strong light penetration, resulting in a conspicuous vertical migration of pteropods (Herut et al., 2000). The high relative abundance of epipelagic pteropod species observed in this study (Figs. 5Ab, Ag, Bb, Bg, Cb, Cg) across the base of the south-eastern Mediterranean margin is consistent with Almogi-Labin and Reiss (1977), who described *C. conica* and *C. acicula* as being the most abundant species in the fraction  $> 63\ \mu\text{m}$  along the Israeli coast. The high dominance of these species and of *H. inflatus* may result from their affinity for deep light penetration and a high tolerance to low-productivity environments (Stubbing, 1938) and, in the case of *Creseis* spp., also their ability to live in very shallow-water habitats as found off Nosy Be, Madagascar (Herman and Rosenberg, 1969; Frontier, 1973). A similar ratio between epipelagic vs. mesopelagic species in the sediments of the Red Sea has been suggested to be a possible indication of the large degree of oxygen deficiency in the oxygen minimum zone (Almogi-Labin et al., 1991, 1998; Singh et al., 2001). A well-developed oxygen minimum zone would restrict the ability of mesopelagic species to survive, promoting the dominance of the epipelagic species (Almogi-Labin et al., 1991, 2008). In the investigated samples the ratio of mesopelagic vs. epipelagic species is fairly constant overall (Fig. 5Ac, Bc, Cc), possibly indicating apparent constant palaeoceanographic conditions in the three areas.

The different reproduction strategy of *H. inflatus* with respect to *Creseis* may explain the observed low abundance of the former in the  $> 63\ \mu\text{m}$  fraction even when it is abundant in the  $> 125\ \mu\text{m}$  fraction. *Heliconoides inflatus* retains the embryos within its mantle until they reach a size of 66–68  $\mu\text{m}$ , and then it releases the free-swimming veliger larvae into the sea (Lalli and Wells, 1973), increasing their

probability of survival. Frontier (1973) suggests that this species is abundant in pelagic environments far from the coast, and this may explain its low present abundances around 40 m from the coastline and higher abundances in the Gal-C channel around 100 km from the coast. However, the prominently high abundance of *H. inflatus* in the coral-transition area, which is the closest to the coast, between 2800 and 3400 BP, in both size fractions ( $> 63$  and  $> 125\ \mu\text{m}$ ), suggests that the oceanic conditions were different off the margin at that time. The mesopelagic *H. inflatus* and the epipelagic *L. trochiformis* and *C. acicula* are regarded as typical upwelling species (Thiede and Jünger, 2019). Upwelling regions are characterized by an oxygen-deficient seafloor resulting from the decay of organic matter (Stein, 1990). Coastal upwelling areas are also characterized by terrigenous detrital fluxes of terrestrial origin (Sarnthein et al., 1982). A recent investigation on modern particulate organic carbon fluxes in the Levantine Basin has demonstrated that today particulate organic matter may arrive at the seafloor by vertical sinking but more frequently by lateral transport due to the impact of terrestrial or shelf processes (Alkalay et al., 2020). High TOC content in the coral area (Fig. 6) coupled with a high abundance of the mesopelagic and upwelling species *H. inflatus* and other Limacinidae between 2800 and 3400 BP (Supplement S1) may suggest a local and coastal upwelling episode at that time or alternatively that the hydrographic conditions varied in narrow, coast-parallel zones, and hence they may rather reflect variations in Nile discharge.

## 5.2 Importance of the investigated size fraction

It is well known that the choice of net and sieve mesh sizes is an important aspect in field sampling and laboratory procedures, respectively (e.g. Wells, 1973). Studies from the Mediterranean Sea (Thiriot-Quievreux, 1968) and the South Atlantic Ocean (Boltovsky, 1971) report that the use of large size nets could underestimate the real numbers of living *H. inflatus* and *Creseis virgula* in the water masses. The overlooking of a large part of the living pteropod population can result in a wrong interpretation of the seasonal data (Wells, 1973). In our results, the significant differences between the ratio of epipelagic vs. mesopelagic species in the size fractions  $> 63$  and  $> 125\ \mu\text{m}$  (Fig. 5) indicate that the exclusive use of the largest  $> 125\ \mu\text{m}$  fraction in pteropod analyses is a severe bias that could cause potential misinterpretations. These may include, for example, underestimation of pteropod relative abundance and species distribution.

In particular, epipelagic species of the genus *Creseis* have an acicular and conical and very fragile elongate shell, susceptible to fragmentation. They are mainly present as thin protoconchs  $< 125\ \mu\text{m}$ , and as such they could be underestimated in comparison to the mesopelagic, larger, and more robust *H. inflatus* (Fig. 5Ae, Af, Be, Bf, Ce, Cf).

Moreover, the relevant numerical abundance of *Creseis* spp. indicates the importance of studying the > 63 µm size fraction (Figs. 5Af; Bf, Cf; Table 2). Our observed differences in abundance between the > 125 and the > 63 µm fractions of *Creseis* spp. are up to 53 % in the coral-transition area, 52 % in the pockmark area, and 63 % in the Gal-C channel area (Fig. 5).

## 6 Conclusions

Here, we have described the pteropods and heteropods (Figs. 4–6) from three sampling locations across the south-eastern Mediterranean continental margin off southern Israel (the coral, pockmark, and Gal-C channel sites) representing different habitats over the past 5800–5300 cal BP. Several differences have been observed in the holoplanktonic pteropod numbers, generally increasing with water depth and distance from the coast and probably reflecting changing levels of interaction with the margin. The primary abundant species observed are consistent with those previously found in the eastern Mediterranean Sea and are associated with temperate to subtropical environments. The observed presence of tropical species may support the suggestion that the eastern Mediterranean constitutes a refugium for these species.

The absence of aragonite dissolution in near-bottom waters in the eastern Mediterranean Sea provides an exceptional opportunity to study the evolution of pteropod assemblages in relation to oceanographic and climatic changes. The relation between *Creseis* spp. and *H. inflatus* is generally constant through the sedimentary record without substantial changes in the total pteropod assemblage composition. This may suggest stable conditions of water masses during the late Holocene. However, between 2800 and 3400 BP a local and coastal upwelling episode may have occurred in the coral area or alternatively the hydrographic conditions varied along narrow, coast-parallel zones, possibly reflecting variations in Nile discharge.

This study highlights the importance of including the smallest fraction (63–125 µm) in studies of pteropod assemblages. Most of the protoconchs of *Creseis* spp. were found in this small size fraction down to a water depth of ~ 1300 m, substantially adding important quantitative and qualitative information and therefore improving the environmental interpretation.

**Data availability.** All data mentioned in the paper are provided as a Supplement (S1 and S2).

**Supplement.** The supplement related to this article is available online at: <https://doi.org/10.5194/jm-42-13-2023-supplement>.

**Author contributions.** SS, AAL, and VB conceived the project. YM was chief scientist on board the cruise and contributed to the interpretation. VB performed the sample processing and pteropod and heteropod picking. VB and AAL performed the species identification. All authors contributed to the interpretation of the data and writing the paper.

**Competing interests.** The contact author has declared that none of the authors has any competing interests.

**Disclaimer.** Publisher's note: Copernicus Publications remains neutral with regard to jurisdictional claims in published maps and institutional affiliations.

**Acknowledgements.** The authors thank the scientific and technical crew of the R/V *Aegaeo* for providing technical support during the cruise. The EUROFLEETS2 SEMSEEP cruise was funded by the European Union FP7 Programme under grant agreement no. 312762. Funding for shore-based investigations, which made this research possible, was provided by the Swiss National Science Foundation (SNSF), grant ref. 200021\_175587. We warmly thank Christoph Neururer, who helped during SEM operations. We thank Sandra Borderie, from the University of Fribourg, for her help in the use of the free software package GMT (Generic Mapping Tools: Wessel and Smith, 1991). Karin Wyss and Negar Haghpor at ETH Zurich are thanked for help with sample preparation and the AMS analysis. We acknowledge the Norwegian Research Council through the project AKMA, Advancing Knowledge of Methane in the Arctic (project number 287869), for funding isotope analyses.

**Financial support.** This research has been supported by the Schweizerischer Nationalfonds zur Förderung der Wissenschaftlichen Forschung (grant no. 200021\_175587), the Norges Forskningsråd (grant no. 287869), and the European Commission, Seventh Framework Programme (EUROFLEETS2 (grant no. 312762)).

**Review statement.** This paper was edited by Francesca Sangiorgi and reviewed by Joachim Schönfeld and one anonymous referee.

## References

- Alkalay, R., Zlatkin, O., Katz, T., Herut, B., Halicz, L., Berman-Frank, I., and Weinstein, Y.: Carbon export and drivers in the southeastern Levantine Basin, Deep-Sea Res. Pt. II, 171, 104713, <https://doi.org/10.1016/j.dsr2.2019.104713>, 2020.
- Almogi-Labin, A.: Stratigraphic and paleoceanographic significance of Late Quaternary pteropods from deep-sea cores in the Gulf of Aqaba (Elat) and northernmost Red Sea, Mar. Micropaleontol., 7, 53–72, [https://doi.org/10.1016/0377-8398\(82\)90015-9](https://doi.org/10.1016/0377-8398(82)90015-9), 1982.

- Almogi-Labin, A.: Population dynamics of planktic Foraminifera and Pteropoda – Gulf of Aqaba, Red Sea, P. Roy. Neth. Acad. Sci. B, 87, 481–511, 1984.
- Almogi-Labin, A. and Reiss, Z.: Quaternary pteropods from Israel, Rev. Española Micropaleontol., 9 5–48, [https://doi.org/10.1016/0031-0182\(86\)90013-1](https://doi.org/10.1016/0031-0182(86)90013-1), 1977.
- Almogi-Labin, A., Hemleben, C., and Deuser, W. G.: Seasonal variation in the flux of euthecosomatous pteropods collected in a deep sediments trap in the Sargasso Sea, Deep-Sea Res. Pt. I, 35, 441–464, [https://doi.org/10.1016/0198-0149\(88\)90020-9](https://doi.org/10.1016/0198-0149(88)90020-9), 1988.
- Almogi-Labin, A., Hemleben, C., Meischner, D., and Erlenkauer, H.: Paleoenvironmental events during the last 13,000 years in the central Red Sea as recorded by pteropoda, Paleoceanography, 6, 83–98, 1991.
- Almogi-Labin, A., Hemleben, C., and Meischner, D.: Carbonate preservation and climatic changes in the central Red Sea during the last 380 kyr as recorded by pteropods, Mar. Micropaleontol., 33, 87–107, 1998.
- Almogi-Labin, A., Edelman-Furstenberg, Y., and Hemleben, C.: Variations in biodiversity of thecosomatous pteropods during the Late Quaternary as a response to environmental changes in the Gulf of Aden-Red Sea-Gulf of Aqaba ecosystems, in: Aqaba-Eilat, the Improbable Gulf, Environment, Biodiversity and Preservation, edited by: Por, D., The Hebrew University Magnes Press, Jerusalem, 31–48, 2008.
- Basso, D., Beccari, V., Almogi-Labin, A., Hyams-Kaphzan, O., Weissman, A., Makovsky, Y., Rueggeberg, A., and Spezzaferri, S.: Macro-and micro-fauna from cold seeps in the Palmahim Disturbance (Israeli off-shore), with description of *Waisiunconcha corsellii* n. sp. (Bivalvia, Vesicomysidae), Deep-Sea Res. Pt. II, 171, 104723, <https://doi.org/10.1016/j.dsr2.2019.104723>, 2020.
- Bè, A. W. H. and Gilmer, R. W.: A zoogeographic and taxonomic review of euthecosomatous Pteropoda, in: Oceanic micropaleontology, edited by: Ramsay A. T. S., Academic Press, New York, 733–808, 1997.
- Beccari, V., Basso, D., Spezzaferri, S., Rüggeberg, A., Neuman, A., and Makovsky, Y.: Preliminary video-spatial analysis of cold seep bivalve beds at the base of the continental slope of Israel (Palmahim Disturbance), Deep-Sea Res. Pt. II, 171, 104664, <https://doi.org/10.1016/j.dsr2.2019.104664>, 2020.
- Behar, F. and Beaumont, V.: Rock-Eval 6 Technology: Performances and Developments, Oil Gas Sci. Tech.-Rev. IFP, 56, 111–134, <https://doi.org/10.2516/ogst:2001013>, 2001.
- Benson, W. H.: Account of *Oxygyrus* a new genus of pelagian shells allied to the genus *Atlanta* of Lesueur, with a note on some other pelagian shells lately taken on board of the ship Malcolm, J. Asiatic Soc. Bengal, 4, 173–176, 1835.
- Berger, W. H.: Deep-sea carbonate: pteropod distribution and the aragonite compensation depth, Deep-Sea Res., 25, 447–452, [https://doi.org/10.1016/0146-6291\(78\)90552-0](https://doi.org/10.1016/0146-6291(78)90552-0), 1978.
- Berger, W. H.: Preservation of Foraminifera, Short Course No. 6, Society Economic, Paleontologists Mineralogists, University of California, 105–155, ISBN 0608056766, 9780608056760, 1979.
- Berner, R. A.: Sedimentation and dissolution of pteropods in the ocean, in: The fate of fossil fuel CO<sub>2</sub> in the oceans, edited by: Andersen, N. R. and Malahoff, A., Springer New York, NY, Plenum Press, 243–260, ISBN 978-1-4899-5018-5, 1977.
- Biekart, J. W.: Euthecosomatous pteropods as paleohydrological and paleoecological indicators in a Tyrrhenian deep-sea core, Palaeogeogr. Palaeoclimatol., 71, 205–224, [https://doi.org/10.1016/0031-0182\(89\)90050-3](https://doi.org/10.1016/0031-0182(89)90050-3), 1989.
- Blanc-Vernet, L., Chamley, H., and Froget, C.: Paleoclimatological analysis of a core from the northwestern Mediterranean. Comparison of the results of three studies: Foraminifera, Pteropoda and sedimentology, Palaeogeogr. Palaeoclimatol., 6, 215–235, [https://doi.org/10.1016/0031-0182\(69\)90015-7](https://doi.org/10.1016/0031-0182(69)90015-7), 1969.
- Bogi, C. and Galil, B. S.: The bathybenthic and pelagic molluscan fauna off the Levantine coast, Eastern Mediterranean, Boll. Malacol., 39, 79–90, 2004.
- Boltovskoy, D.: Pteropodos thecosomados del Atlantico suboccidental, Malacologia, 11, 121–140, 1971.
- Bosc, L. A. G.: Histoire naturelle des coquilles, contenant leur description, les mœurs des animaux qui les habitent et leurs usages, Deterville, Paris, 1, 343; 2, 330; 3, 292; 4, 280; 5, 255, de Crapelet, Deterville, Paris, <https://doi.org/10.5962/bhl.title.51350>, 1801.
- Brady, H. B.: Supplementary note on the foraminifera of the Chalk of the New Britain group, Geol. Mag., 4, 534–536, 1877.
- Buccheri, G. and Torelli, L.: Stratigraphy and paleoclimatic evolution of the cores BS-77-15 and BS77-33 (Sardinia Basin, Western Tyrrhenian Sea by mean of pteropod assemblages, Acta Naturalia de l'Ateneo Parmense, 17, 73–94, 1981.
- Cita, M. B. and Zocchi, M.: Distribution patterns of benthic foraminifera on the floor of the Mediterranean Sea, Oceanol. Acta, 1, 445–462, 1978.
- Clarke, K. R. and Gorley, R. N.: Getting started with PRIMER v7, PRIMER-E: Plymouth, Plymouth Marine Laboratory, 20, 2015.
- Coleman, D. F., Austin Jr., J. A., Ben-Avraham, Z., Makovsky, Y., and Tchernov, D.: Seafloor pockmarks, deep water corals, and cold seeps along the continental margin of Israel, Oceanography 25, 40–41, 2012.
- Corselli, C. and Grecchi, G.: Considerazioni su di una popolazione di *Cavolinia gibbosa gibbosa* del Mediterraneo orientale, Boll. Malacol., 23, 83–91, 1987.
- Corselli, C. and Grecchi, G.: Considerazioni sui Thecosomata attuali del Bacino Mediterraneo, Lavori della Società Italiana di Malacologia, 24, 120–130, 1990.
- de Blainville, H. M. D.: Hyale, Hyalæa (Malacoz.), in: Dictionnaire des Sciences Naturelles, Levrault, edited by: Cuvier, F., Strasbourg and Le Normant, Paris, 22, 65–83, 1821.
- Dessandier, P. A., Borrelli, C., Yao, H., Sauer, S., Hong, W. L., and Panieri, G.: Foraminiferal  $\delta^{18}\text{O}$  reveals gas hydrate dissociation in Arctic and North Atlantic Ocean sediments, Geo-Mar. Lett., 40, 1–17, <https://doi.org/10.1007/s00367-019-00635-6>, 2020.
- de Vera, A. and Seapy, R. R.: *Atlanta selvagensis*, a new species of heteropod mollusc from the Northeastern Atlantic Ocean: (Gastropoda: Carinarioidea), Vieraea, 34, 45–54, 2006.
- d'Orbigny, A. D.: Voyage dans l'Amérique méridionale (le Brésil, la république orientale de l'Uruguay, la République argentine, la Patagonie, la République du Chili, la République de Bolivie, la République du Pérou), exécuté pendant les années 1826, 1827, 1828, 1829, 1830, 1831, 1832 et 1833, Tome 5(3) Mollusques, i–xliii, 1–758, 1835.
- Eschscholtz, J. F.: Zoologischer Atlas, enthaltend Abbildungen und Beschreibungen neuer Thierarten, während des Flottcapitains von Kotzebue zweiter Reise um die

- Welt, auf der Russisch-Kaiserlichen Kriegsschlupf Predpriaetië in den Jahren 1823–1826, Reimer, Berlin, 1–18, <https://doi.org/10.5962/bhl.title.152182>, 1829.
- Frontier, S.: Zooplancton de la région de Nosy-Bé, VI. Ptéropodes, Hétéropodes—première partie: espèces holonéritiques et néritiques-internes, Cahiers ORSTOM, Océanography, 11, 273–289, 1973.
- Furnestin, M. L.: Aspects of the zoogeography of the Mediterranean plankton, Zoogeography and diversity of Plankton, Halsted Press, University of California, 5, 191–253, ISBN 0470267984, 9780470267981, 1979.
- Garfunkel, Z., Arad, A., and Almagor, G.: The Palmahim disturbance and its regional setting, Geol. Surv. Israeli Bull., 72, 1–56, 1979.
- Gertman, I., Zodiatis, G., Ozer, T., Goldman, R., and Herut, B.: Renewal of deep water in vicinity of the Eastern Levantine slope, Rapport Commission Internationale Mer Méditerranée, 41, 1–124, 2016.
- Giamali, C., Kontakiotis, G., Koskeridou, E., Ioakim, C., and Antonarakou, A.: Key Environmental Factors Controlling Planktonic Foraminiferal and Pteropod Community's Response to Late Quaternary Hydroclimate Changes in the South Aegean Sea (Eastern Mediterranean), J. Mar. Sci. Eng., 8, 709, <https://doi.org/10.3390/jmse8090709>, 2020, 2020.
- Gómez, F., González, N., Echevarría, F., and García, C. M.: Distribution and Fluxes of Dissolved Nutrients in the Strait of Gibraltar and its Relationships to Microphytoplankton Biomass, Estuar. Coast. Shelf Sci., 51, 439–449, <https://doi.org/10.1006/ecss.2000.0689>, 2000.
- Gray, J. E.: Figures of molluscos animals, selected from various authors, edited by: Gray, M. E., Longman, Brown, Green and Longmans, London, 4, 219, <https://doi.org/10.5962/bhl.title.10461>, 1850.
- Grecchi, G.: Molluschi planctonici e bentonici in sedimenti sapropelitici del Quaternario della Dorsale Mediterranea, Boll. Malacol., 20, 1–34, 1984.
- Grecchi, G. and Bertolotti, M.: Interpretazione paleoclimatica della carota CG18-BAN82 basata sull'analisi di Thecosomata Euthecosomata del Quaternario del Mediterraneo orientale, Boll. Mus. Reg. Sci. Nat. Torino, 6, 73–132, 1988.
- Gvritzman, Z., Reshef, M., Buch-Leviatan, O., Groves-Gidney, G., Karcz, Z., Makovsky, Y., and Ben-Avraham, Z.: Bathymetry of the Levant Basin: interaction of salt-tectonics and surficial mass movements, Mar. Geol., 360, 25–39, <https://doi.org/10.1016/j.margeo.2014.12.001>, 2015.
- Heaton, T. J., Köhler, P., Butzin, M., Bard, E., Reimer, R. W., Austin, W. E. N., Bronk Ramsey, C., Grootes, P. M., Hughen, K. A., Kromer, B., Reimer, P. J., Adkins, J. F., Burke, A., Cook, M. S., Olsen, J., and Skinner, L. C.: Marine20 – the marine radiocarbon age calibration curve (0–55,000 cal BP), Radiocarbon, 62, <https://doi.org/10.1017/RDC.2020.68>, 2020.
- Hennekam, R.: High-frequency climate variability in the late Quaternary Eastern Mediterranean: Associations of Nile discharge and Basin overturning circulation dynamics (Doctoral dissertation, Utrecht Studies in Earth Science, Department of Earth Sciences), 78, 2015.
- Herman, Y.: Paleoclimatic and paleohydrologic record of Mediterranean deep-sea cores based on pteropods, planktonic and benthonic foraminifera, Rev. Española Micropaleontol., 13, 171–200, 1981.
- Herman, Y. and Rosenberg, P. E.: Pteropods as bathymetric indicators, Mar. Geol., 7, 169–173, [https://doi.org/10.1016/0025-3227\(69\)90039-5](https://doi.org/10.1016/0025-3227(69)90039-5), 1969.
- Herut, B., Almogi-Labin, A., Jannink, N., and Gertman, I.: The seasonal dynamics of nutrient and chlorophyll-a concentration on the SE Mediterranean shelf-slope, Oceanol. Acta, 23, 771–782, [https://doi.org/10.1016/S0399-1784\(00\)01118-X](https://doi.org/10.1016/S0399-1784(00)01118-X), 2000.
- Hyams-Kaphzan, O., Lubinevsky, H., Crouvi, O., Harlavan, Y., Herut, B., Kanari, M., Tom, M., and Almogi-Labin, A.: Live and dead deep-sea benthic foraminiferal macrofauna of the Levantine Basin (SE Mediterranean) and their ecological characteristics, Deep-Sea Res. Pt. I, 136, 72–83, <https://doi.org/10.1016/j.dsr.2018.04.004>, 2018.
- Janssen, A. W.: Quaternary to Recent holoplanktonic Mollusca (Gastropoda) from bottom samples of the Eastern Mediterranean Sea: systematics, morphology, Boll. Malacol., 48, 1–105, 2012.
- Janssen, A. W. and Peijnenburg, K. T.: Holoplanktonic Mollusca: development in the Mediterranean Basin during the last 30 million years and their future, The Mediterranean Sea, Springer, Dordrecht, 341–362, ISBN 9789400767034, 2014.
- Johnson, R., Manno, C., and Ziveri, P.: Spring distribution of shelled pteropods across the Mediterranean Sea, Biogeosciences Discuss. [preprint], <https://doi.org/10.5194/bg-2020-53>, 2020.
- Katz, O., Ashkenazi, L., Sultan-Levi, S., Abramovich, S., Almogi-Labin, A., and Hyams-Kaphzan, O.: Characterization of recent deep-sea debris in the Eastern Mediterranean based on foraminiferal taphonomy, Geol. Soc. Lond. Spec. Publ., 500, 377–391, <https://doi.org/10.1144/SP500-2019-170>, 2020.
- Lalli, C. M. and Wells Jr., F. E.: Brood protection in an epipelagic thecosomatous pteropod, *Spiratella* (“*Limacina*”) *inflata* (D’Orbigny), Bull. Mar. Sci., 23, 933–941, 1973.
- Lesueur, C. A.: Mémoire sur quelques nouvelles espèces d’animaux mollusques et radiaires recueillis dans la Méditerranée près de Nice, Nouveau Bull. Sci. Soc. Phil. Paris, 3, 281–285, 1813.
- Lesueur, C. A.: Mémoire sur deux nouveaux genres de mollusques, Atlante et Atlas, J. Phys. Chim. Hist. Nat., 85, 390–393, 1817.
- Linnaeus, C.: Systema naturae, per regna tria naturae, secundum classes, ordines, genera, species, cum caracteribus, differentiis, synonymis, locis, Editio duodecima, reformata, I, 2, 533–1327, <https://doi.org/10.5962/bhl.title.559>, 1767.
- Makovsky, Y., Rüggeberg, A., Bialik, O., Foubert, A., Almogi-Labin, A., Alter, Y., Bampas, V., Basso, D., Feenstra, E., Fentimen, R., Friedheim, O., Hall, E., Hazan, O., Herut, B., Kallergis, E., Karageorgis, A., Kolountzakis, A., Manousakis, L., Nikolaidis, M., Pantazoglou, F., Rahav, E., Renieris, P., Schleinkofer, N., Sisma Ventura, G., Stasnios, V., Weissman, A., and the EU-ROFLEETS2 SEMSEEP participants: South East Mediterranean SEEP Carbonate, R/V AEGAE0, Cruise EU-ROFLEETS2 SEMSEEP, 20 September–1 October 2016, Piraeus (Greece) – Piraeus (Greece) Cruise Summary Report, 1–62, 2016.
- Malanotte-Rizzoli, P., Artale, V., Borzelli-Eusebi, G. L., Brenner, S., Crise, A., Gacic, M., Kress, N., Marullo, S., Ribera d’Alcalà, M., Sofianos, S., Tanhua, T., Theocharis, A., Alvarez, M., Ashkenazy, Y., Bergamasco, A., Cardin, V., Carniel, S., Civitarese, G., D’Ortenzio, F., Font, J., Garcia-Ladona, E., Garcia-Lafuente, J. M., Gogou, A., Gregoire, M., Hainbucher, D., Kontoyannis, H., Kovacevic, V., Kraskapoulou, E., Kroskos, G., Incarbona, A.,

- Mazzocchi, M. G., Orlic, M., Ozsoy, E., Pascual, A., Poulain, P.-M., Roether, W., Rubino, A., Schroeder, K., Siokou-Frangou, J., Souvermezoglou, E., Sprovieri, M., Tintoré, J., and Triantafyllou, G.: Physical forcing and physical/biochemical variability of the Mediterranean Sea: a review of unresolved issues and directions for future research, *Ocean Sci.*, 10, 281–322, <https://doi.org/10.5194/os-10-281-2014>, 2014.
- Mojtahid, M., Manceau, R., Schiebel, R., Hennekam, R., and De Lange, G. J.: Thirteen thousand years of southeastern Mediterranean climate variability inferred from an integrative planktic foraminiferal-based approach, *Paleoceanography*, 30, 402–422, <https://doi.org/10.1002/2014PA002705>, 2015.
- Molnár, M., Janovics, R., Major, I., Orsovski, J., Gönczi, R., Veres, M., Leonard, A. G., Castle, S. M., Lange, T. E., Wacker, L., Hajdas, I., and Jull, A. J. T.: Status report of the new AMS 14C sample preparation lab of the Hertelendi Laboratory of Environmental Studies (Debrecen, Hungary), *Radiocarbon*, 55, 665–676, <https://doi.org/10.1017/S0033822200057829>, 2013.
- Nemec, M., Wacker, L., Hajdas, I., and Gaggeler, H.: Alternative methods for cellulose preparation for AMS measurement, *Radiocarbon*, 52, 1358–1370, <https://doi.org/10.1017/S0033822200046440>, 2010.
- Niebuhr, C.: Icones rerum naturalium, quas in itinere orientali de pingi curavit Petrus Forskål, prof. Haun., post mortem auctoris, edidit: Niebuhr, C., Hauniae, Copenhagen, Möller, 1–15, 1776.
- Ozer, T., Gertman, I., Kress, N., Silverman, J., and Herut, B.: Interannual thermohaline (1979–2014) and nutrient (2002–2014) dynamics in the Levantine surface and intermediate water masses, SE Mediterranean Sea, *Glob. Plan. Changes*, 151, 60–67, <https://doi.org/10.1016/j.gloplacha.2016.04.001>, 2017.
- Ozer, T., Gertman, I., Gildor, H., Goldman, R., and Herut, B.: Evidence for recent thermohaline variability and processes in the deep water of the Southeastern Levantine Basin, Mediterranean Sea, *Deep-Sea Res. Pt. II*, 171, 104651, <https://doi.org/10.1016/j.dsr2.2019.104651>, 2020.
- Pierrot-Bults, A. C. and Peijnenburg K. T. C. A.: Pteropods, in: *Encyclopedia of marine geosciences*, edited by: Harff, J., Meschede, M., Petersen, S., and Thiede, J., Springer, 1–10, [https://doi.org/10.1007/978-94-007-6644-0\\_88-1](https://doi.org/10.1007/978-94-007-6644-0_88-1), 2015.
- Quoy, J. R. C. and Gaimard, J. P.: Observations zoologiques faites à bord de l’Astrolabe, en mai 1826, dans le Détroit de Gibraltar, *Ann. Sci. Naturell.*, Féruss, XII, 1–145, 1827.
- Rampal, J.: Biogéographie méditerranéenne d’après l’étude des Thecosomes (Mollusques pélagiques), *Journée études Systematique et Biogéographique Méditerranée*, Cagliari, Commission Internationale Exploration Scientifique Mer Méditerranée, 45–54, 1980.
- Ramsey C.: OxCal 4.4, Electronic document, <https://c14.arch.ox.ac.uk/oxcal.html> (last access: 15 March 2023), 2021.
- Rang, S.: Notice sur quelques mollusques nouveaux appartenant au genre Cléodore, et établissement et monographie des sous-genre *Créseis*, *Ann. Sci. Nat.*, 13, 302–319, 1828.
- Roether, W., Klein, B., Manca, B. B., Theocharis, A., and Kioroglou, S.: Transient Eastern Mediterranean deep waters in response to the massive dense-water output of the Aegean Sea in the 1990s, *Prog. Oceanogr.*, 74, 540–571, <https://doi.org/10.1016/j.pocean.2007.03.001>, 2007.
- Rubin-Blum, M., Antler, G., Turchyn, A. V., Tsadok, R., Goodman-Tchernov, B. N., Shemesh, E., Austin, J. A., Coleman, D. F., Makovsky, Y., Sivan, O., and Tchernov, D.: Hydrocarbon-related microbial processes in the deep sediments of the Eastern Mediterranean Levantine Basin, *FEMS Microbiol. Ecol.*, 87, 780–796, <https://doi.org/10.1111/1574-6941.12264>, 2014.
- Rzehak, A.: Die Foraminiferen Fauna der Neogenformation der Umgebung von Mähr-Ostrau, *Verhandlungen des naturforschenden Vereines in Brünn*, 24, 77–126, 1886.
- Sarnthein, M., Thiede, J., Pflaumann, U., Erlenkauser, H., Fütterer, D., Koopmann, B., Lange, H., and Seibold, E.: Atmospheric and oceanic circulation patterns off Northwest Africa during the past 25 million years, in: *Geology of the Northwest African Continental Margin*, edited by: Von Rad, U., Hinz, K., Sarnthein, M., and Seibold, E., Springer, Berlin, Heidelberg, 545–604, [https://doi.org/10.1007/978-3-642-68409-8\\_24](https://doi.org/10.1007/978-3-642-68409-8_24), 1982.
- Singh, A., Ramachandran, K., Samsuddin, M., Nisha, N., and Haneeshkumar, V.: Significance of pteropods in deciphering the late Quaternary sea-level history along the southwestern Indian shelf, *Geo-Mar. Lett.*, 20, 243–252, <https://doi.org/10.1007/s003670000056>, 2001.
- Sisma-Ventura, G., Bialik, O. M., Makovsky, Y., Rahav, E., Ozer, T., Kanari, M., Marmen, S., Blekin, N., Guy-Haim, T., Antler, G., and Herut, B.: Cold seeps alter the near-bottom biogeochemistry in the ultraoligotrophic Southeastern Mediterranean Sea, *Deep-Sea Res. Pt. I*, 83, 103744, <https://doi.org/10.1016/j.dsr.2022.103744>, 2022.
- Smith, E. A.: Report on the Heteropoda collected by HMS Challenger during the years 1873–1876, Report on the Scientific Results of the Voyage of H. M. S. Challenger during the years 1873–76, Johnson Reprint Company Ltd., Zoology, 23, 1–51, 1888.
- Spiro, B., Ezra, O., Najorka, J., Delgado, A., Bialik, O., Ben-Avraham, Z., Coleman, D., and Makovsky, Y.: Mineralogical, chemical and stable C and O isotope characteristics of surficial carbonate structures from the Mediterranean offshore Israel indicate microbial and thermogenic methane origin, *Geo-Mar. Lett.*, 41, 1–17, <https://doi.org/10.1007/s00367-021-00684-w>, 2021.
- Stein, R.: Accumulation of Organic Carbon in Marine Sediments, *Lecture Notes in Earth Sciences*, 34, Springer, New York, ISBN 978-0387538136, 1990.
- Stubbing, H. G.: Pteropoda, *Sci. Rep.*, John Murray Expedition 5, 15–33, 1938.
- Synal, H.-A., Stocker, M., and Suter, M.: MICADAS: A new compact radiocarbon AMS system. *Nuclear Instruments and Methods in Physics Research Section B: Beam Interactions with Materials and Atoms, Accelerator Mass Spectrometry*, 259, 7–13, <https://doi.org/10.1016/j.nimb.2007.01.138>, 2007.
- Thiede, J. and Jünger, B.: Faunal and floral indicators of ocean coastal upwelling (NW African and Peruvian continental margins), in: *Upwelling systems: Evolution since the Early Miocene*, edited by: Summerhayes, C. P., Prell, W. L., and Emeis, K. C., *Geol. Soc. Spec. Publ.*, 64, 47–76, <https://doi.org/10.1144/GSL.SP.1992.064.01>, 1992.
- Thiriou-Quievreux, C.: Variations saisonnières des mollusques dans le plancton de la région de Banyuls-sur-Mer (zone Sud du Golfe de Lion) novembre 1965–décembre 1967, *Vie Milieu Sér. B*, 20, 35–83, 1968.
- Van der Spoel, S.: Euthecosomata, a group with remarkable developmental stages (Gastropoda-Pteropoda), Brill, 1–375, ISBN 978-90-04-07153-7, 1967.

- Vinogradov, M. Y. E.: Food sources for the deep-water fauna, Speed of decomposition of dead Pteropoda, *Doklady Akademii Nauk SSSR*, 138, 1439–1442, 1961.
- Violanti, D., Grecchi, G., and Castradori, D.: Paleoenvironmental interpretation of Core BAN88-11GC (Eastern Mediterranean, Pleistocene-Holocene), on the grounds of Foraminifera, Thecosoma and Calcareous Nannofossils, *Il Quaternario*, 4, 13–39, 1991.
- Waldman, R., Brüggemann, N., Bosse, A., Spall, M., Somot, S., and Sevault, F.: Overturning the Mediterranean Thermohaline Circulation, *Geophys. Res. Lett.*, 45, 8407–8415, <https://doi.org/10.1029/2018GL078502>, 2018.
- Wall-Palmer, D., Smart, C. W., Hart, M. B., Leng, M. J., Borghini, M., Manini, E., Aliani, S., and Conversi, A.: Late Pleistocene pteropods, heteropods and planktonic foraminifera from the Caribbean Sea, Mediterranean Sea and Indian Ocean, *Micropaleontology*, 60, 557–578, 2014.
- Wall-Palmer, D., Smart, C. W., Kirby, R., Hart, M. B., Peijnenburg K. T. C. A., and Janssen A. W.: A review of ecology, palaeontology and distribution of atlantid heteropods (Caenogastropoda: Pterotracheoidea: Atlantidae), *J. Molluscan Stud.*, 82, 221–234, <https://doi.org/10.1093/mollus/eyv063>, 2016.
- Wall-Palmer, D., Janssen, A. W., Goetze, E., Choo, L. Q., Mekkes, L., and Peijnenburg, K. T. C. A.: Fossil-calibrated molecular phylogeny of atlantid heteropods (Gastropoda, Pterotracheoidea), *BMC Evol. Biol.*, 20, 124, <https://doi.org/10.1186/s12862-020-01682-9>, 2020.
- Weikert, H.: Plankton and the pelagic environment, in *Red Sea, Red Sea, Key environments*, edited by: Edwards, A. J. and Head, S. M., Pergamon Press, Oxford, 90–111, 1987.
- Wells, F. E.: Effects of mesh size on estimation of population densities of tropical euthecosomatous pteropods, *Mar. Biol.*, 20, 347–350, <https://doi.org/10.1007/BF00354276>, 1973.
- Wessel, P., Smith, W. H. F., Scharroo, R., Luis, J., and Wobbe, F.: *Generic Mapping Tools: Improved version Released*, EOS Trans. AGU, 94, 409–410, <https://doi.org/10.1002/2013EO450001>, 2013.
- Wormuth, J. H.: Vertical distributions and diel migrations of Euthecosomata in the northwest Sargasso Sea, *Deep-Sea Res. Pt. A*, 28, 1493–1515, [https://doi.org/10.1016/0198-0149\(81\)90094-7](https://doi.org/10.1016/0198-0149(81)90094-7), 1981.